THERMAL PROPERTIES OF A SUSTAINABLE CEMENT MATERIAL: EFFECT OF CURE CONDITIONS

#TANIA DEY

Department of Materials and Chemistry, Faculty of Engineering, Free University of Brussels, Pleinlaan 2, 1050 Brussels, Belgium

#E-mail: taniadey@hotmail.com

Submitted July 19, 2014; accepted December 19, 2014

Keywords: Calcium phosphate cement, Curing, Cement hydration, Thermal properties, Activation energy

This paper presents the effect of cure temperature and cure time on the thermal properties of wollastonite-based calcium phosphate cement, a sustainable cement material. Mass losses of 11.7 % at 105 - 220°C and 1.8 % at 380 - 500°C in TGA experiment were attributed to brushite to monetite and monetite to calcium pyrophosphate conversion, respectively; which was further confirmed by FTIR. TGA results also indicated that the mass loss can be minimized by increasing curing time and decreasing curing temperature. Deformation values recorded from the first heating cycle of TMA results revealed a linearly decreasing trend with increase in curing time. CTE values, as obtained from the second heating cycle of TMA results remained more-or-less constant with variation in curing time and slightly increased with increase in cure temperature, possibly due to change in moisture content. From the (exothermic) DSC curves, the rate of hydration at different cure temperatures were evaluated using the linear slope in the accelerating period of cement hydration and the data was matched with a model-free Freidman analysis. The activation energy was found to be 57.8 kJ·mol^{-1}.

INTRODUCTION

Legend says that the reason why Charles Bridge in Prague withstood 600 years of wheeled traffic (until it was made pedestrian only) and occasional flooding is that egg yolk was mixed into the mortar to strengthen the construction. Similarly myriads of materials occur in nature, which can serve one purpose or another, in preparing construction materials. Pozzolanic material (e.g. volcanic ash, fly ash, metakaolin, slag) based Geopolymer, which dates back to ancient Roman civilization and great pyramids of Egypt, is sustainable and is a good alternative to conventional cements [1-3]; due to its greater strength, greater road-salt and acid resistance, lower setting time (48 hours vs. 28 days), and less carbon footprint. It even holds promise of replacing the existing Portland cement. Natural mineral (e.g. Wollastonite) based Inorganic Phosphate Cements (IPC) is not so well studied [4, 5] and is another sustainable alternative to conventional cement materials.

IPC belongs to the generic group of Calcium Phosphate Cements (CPC), which are commonly used in restorative dentistry and orthopedic bone substitution [6-14], often times further reinforced with polymeric microparticles [15, 16] or fibers [17, 21]. The wollastonite-phosphate cement in this study is an example of a ceramic composite having superior strength, fire retardant and weather resistant properties, and the potential to offer self-healing effect towards crack repair by means of a remineralized surface layer [22].

The advantages of Wollastonite-based cement materials are mainly threefold. The precursor, Wollastonite is a natural mineral found in guano-rich caves, hence sustainable. It is believed to be a precursor of apatite, formed by guano-initiated metamorphic reaction of calcite (limestone) and clay (silica) at a low pH.

$$SiO_2 + CaCO_3 = CaSiO_3 + CO_2$$

Besides, the Wollastonite-based IPC matrix shows a neutral pH after hardening, so glass fibers (e.g. E-glass) can be used for reinforcement, in contrary to conventional cement. Moreover, this kind of mould can resist high temperature (above 200°C) during processing, without giving off toxic gases.

Previous studies suggest that IPC is not stable, due to transformation of the material when it is exposed to elevated temperatures. One way to stabilize IPC is through hydrothermal post curing. This technique is based on thermally induced transformation of the unstable calcium phosphate phases into more stable phases resulting in minimization of shrinkage, by deliberately leaving sufficient pore moisture [5]. A different approach is to obtain a stable IPC material by optimizing the curing process.

Volume change is the most detrimental property of cement causing shrinkage, which affects long-term strength and durability. 'Shrinkage' mechanism can be varied: a) plastic shrinkage b) drying shrinkage c) autogenous shrinkage d) carbonation shrinkage (see http://aboutcivil.com/shrinkage-in-concrete.html). To avoid shrinkage, it is necessary to optimize the curing (means hardening or setting in the context of concretes) condition during IPC production.

This paper reports the effect of curing condition (curing temperature and curing time) on thermal properties of Wollastonite based IPC. The curing temperatures (30, 40, 50, 60 and 80°C) as well as in curing times (24, 48 and 72 h) were varied to study its effect on IPC specimens. The main experimental techniques used in this investigation were Thermo Gravimetric Analyzer (TGA), Thermo Mechanical Analyzer (TMA), Differential Scanning Calorimetry (DSC) and Infra Red spectroscopy (IR), which can be further complemented with some imaging techniques.

EXPERIMENTAL

Materials and methods

Inorganic phosphate cement is a mixture of calcium silicate powder (e.g. Wollastonite, $CaSiO_3$) and phosphoric acid based solution of metal oxides, in a retardant fluid namely borax solution (proprietary formulation). If the molar ratio of phosphoric acid and Wollastonite powder is in between 0.39 and 1.00, only one type of calcium phosphate (Brushite, $CaHPO_4{,}2H_2O$) is formed [4]:

$$CaSiO_3 + H_3PO_4 + (1 + x)\, H_2O \rightarrow$$
$$\rightarrow CaHPO_4 \cdot 2H_2O + SiO_2 \cdot xH_2O$$

If the molar ratio is 1.00, Brushite as well as Monetite ($CaHPO_4$) are formed.

The calcium silicate powder, Wollastonite (median particle size 15 μm and BET surface area 1.1 $m^2 \cdot g^{-1}$) was obtained from NYCO Minerals Inc. Willsboro, NY; which originally came from the Sonoran desert of Mexico. Wollastonite retains its acicular or needle-like structure in the ceramic, as the reaction occurs between the surface of whisker and matrix, but very fine powders of Wollastonite may completely react loosing their shape [23].

Sample preparation

The weight ratio of the fluid (phosphoric acid based solution of metal oxides in retardant fluid) to the powder (calcium silicate powder, referred as m200st in this paper) was kept 1 : 0.8. The components were mixed using a Heidolph overhead stirrer RZR 2102 control. The mixing was performed in two stages starting at a speed of 500 rpm (for 1 min) and was continued for another minute at 2000 rpm. After that the mixture was left unperturbed, so that the entrapped air bubbles can move up. A batch of 200 g was prepared each time, providing enough IPC for 6 moulds. The dimensions of the moulds were 50 ×50 × 5 mm.

Curing process

The curing process contained two stages. During the first 24 hours the specimens were covered with a plastic foil, in order to prevent evaporation and kept at room temperature (ERT). Post curing was performed at 60°C for 24 hours in closed condition. The fresh mixture specimen was cured in between the 5 mm gap of two aluminium plates of 150 × 500 × 15 mm dimension, pre-heated to the respective curing temperatures. This ensured better temperature control, less deformation and shiny look in the moulds.

Thermogravimetric analyzer (TGA)

Thermogravimetric Analyzer TGA Q5000 from TA Instruments was used. Samples were heated from 50 to 500°C at a heating rate of 10°C per min under nitrogen. Crushed powders of the cured IPC moulds with an average weight of 50 mg were taken in reusable stainless steel carriers (or bails). Each experiment was performed in triplicate. The results were analyzed by TA Instruments Universal Analysis 2000 software.

Thermal mechanical analyzer (TMA)

TMA is a method for measuring deformation of a material as a function of either temperature or time, by varying the temperature of the material according to a calibrated program, under a non-vibrating load. A Perkin Elmer DMA 7 Dynamical Mechanical Analyzer with Pyris Software, equipped with air purging, was used in TMA mode. A parallel plate disc geometry with a diameter of 5 mm was used, the static force being 100 mN. Heat-cool-heat cycles were performed from 25 to 300°C at the rate of 5°C per min. The cured IPC samples had a height of 5 mm. Each experiment was performed in triplicate. The results were analyzed by TA Instruments Universal Analysis 2000 software.

Differential scanning calorimetry (DSC)

Isothermal tests were carried out in a differential scanning calorimeter DSC822e METTLER TOLEDO with MultiStar HSS7 sensor. The electrical signal represented the difference in heat flux between the two pans, one containing the test sample and the other one being empty. Fresh IPC mixtures in same reaction ratio were sealed inside high pressure stainless steel pans and the desired curing temperature was maintained throughout the experiment. The exothermic reaction of the sample

was visualized as a curve of heat flux against time. Each experiment was performed in triplicate. The results were analyzed by TA Instruments Universal Analysis 2000 software.

InfraRed (IR) spectroscopy

Compounds were identified by FTIR/ATR analysis using a Nicolet 6700 Infrared Spectrometer from Thermo Scientific, fitted with OMNIC software. The absorbance spectra were collected using 32 scans at a resolution of 4 cm^{-1}.

Calculation of activation energy for cement hydration reaction

The rate of chemical reactions is generally known to increase with an increase in temperature, often times represented by Arrhenius equation as follows:

$$ln\,(k) = ln\,(A) - \frac{E_a}{RT} \quad (1)$$

The rate constant, k, in Equation (1) is given in [W], if heat evolution is considered. The parameter, A, is a proportionality constant or pre-exponential factor for the reaction. E_a [J mol^{-1}] refers to the activation energy, R [J·$mol^{-1}K^{-1}$] is the universal gas constant and T [K] is the temperature at which the reaction is occurring. E_a of a system can be calculated by plotting the values of ln(k) against (1/T). The slope of equation (1), - E_a/R, should follow a linear trend, i.e. $y = mx + c$, and thereby will allow for the determination of E_a. The pre-exponential factor ln(A) is then obtained from the y-axis intercept.

Friedman analysis, as given by equation (2), can be used to assess the change in apparent activation energy during the progress of a reaction [24], and is also based on the Arrhenius equation. Friedman analysis can be used either as model-free, i.e. when ($A/f(\alpha)$) is considered as a constant, or model-based when combined with a specific function for f (α), as in Avrami-Erofeev model.

$$ln\left(\frac{D\alpha}{dt}\right) = ln\left(\frac{A}{f(\alpha)}\right) - \frac{E_a}{RT} \quad (2)$$

The rate of advancement, ($d\alpha/dt$) of hydrate precipitation can be expressed in terms of fractional degree of hydration or precipitation, α, which is defined by the ratio of heat liberated during a specific period of time, t. In equation (3) for α, Q represents the heat evolved at a given time, where Q_i and Q_f are the initial and final values, respectively.

$$\alpha = \frac{Q_i - Q}{Q_i - Q_f} \quad (3)$$

Avrami-Erofeev model is given by Equation (4), where α is the degree of hydration and the parameter m is a constant which depends on the morphology of crystal formed [25].

$$f(\alpha) = m\,(1 - \alpha)\,[-\,ln\,(1 - \alpha)]^{(m-1)/m} \quad (4)$$

Instead of Avrami-Erofeev model, model-free Friedman analysis was used in this study, which is also capable of providing E_a values up to a good approximation.

RESULTS AND DISCUSSIONS

TGA results (Figure 1a, two curing temperatures shown only) show that mass loss can be minimized by increasing the curing time. Two dehydration steps in TGA curve in between 105 - 220°C, as obtained from the first derivative (Figure 1b), was indicative of brushite to monetite conversion, which was more pronounced for samples cured at 40°C (Figure 1a). The loss of bound water during this conversion resulted in a mass loss of 11.7 %. TGA results (Figure 1a) also indicate that mass loss can be minimized by decreasing the curing temperature.

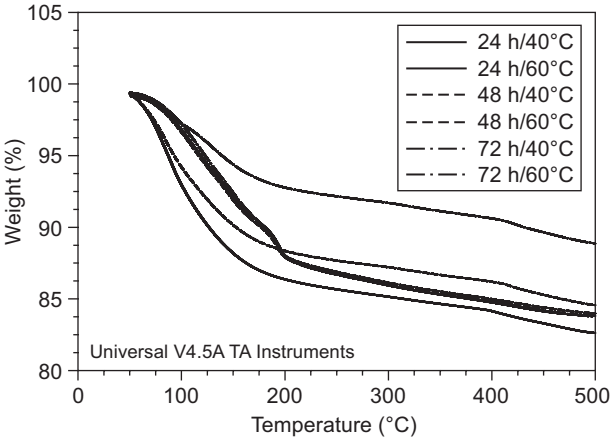

Figure 1a. TGA profile of IPC samples varying in curing temperature (only 40°C and 60°C are shown) and curing time (24, 48 and 72 h); solid line: 24 h, sort dash: 48 h, dash dot: 72 h; black: 40°C, grey: 60°C.

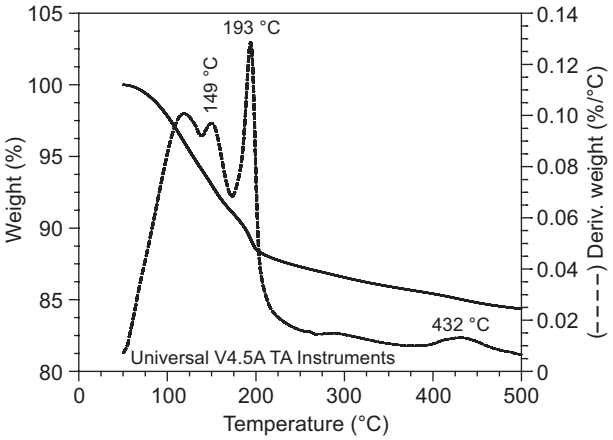

Figure 1b. TGA curve of an IPC material cured at 40°C for 72 h showing steps of dehydration.

Decomposition of monetite ($CaHPO_4$) to calcium pyrophosphate ($Ca_2P_2O_7$) with a mass loss of 1.8 % in the range of 380 - 500°C was also observed in the TGA profile (Figure 1b), which is in good agreement with literature [5].

IR spectra (Figure 2) confirms brushite ($CaHPO_4 \cdot 2H_2O$) to monetite ($CaHPO_4$) conversion accompanied by loss of structural water. Two broad doublets, one at 3538 and 3480 cm^{-1} and the other at 3275 and 3170 cm^{-1} can be attributed to two different kinds of water molecules. The band at 1651 cm^{-1} corresponds to bending mode of OH^- group. The broad little hump at 1399 cm^{-1} is associated with monetite.

Deformation values recorded from the first heating cycle of TMA results [Figure 3, 60°C cure condition shown only] revealed a linearly decreasing trend with increase in curing time. Deformation was also reduced to some extent due to increase in cure temperature (not shown), namely a 20°C increase in curing temperature reduced the deformation by 0.77 %. The values of Coefficient of Thermal Expansion (CTE) were calculated (Table 1) from the slope of the linear curve obtained in the second heating cycle of TMA experiments. An increase in curing temperature seems to increase the CTE, although it remains more-or-less constant with variation in curing time.

As long as mix proportion, water-cement ratio, concrete age and number of heat-cool cycle remains invariant, which is the case here, the change in CTE can be attributed to change in moisture content. Cement paste is considered as a colloidal amorphous gel with three types of water present in it: (i) water of constitution (chemically bound) (ii) gel water (bound by physical forces) (iii) capillary water (free water inside pores) [26]. Concrete CTE is affected by the availability of moisture in capillary and gel pores. The capillary pores are filled with hydration products and their volume decreases at an early age of the concrete, whereas gel pore volume increases as more gel is formed. Variation of the concrete CTE due to hydration and moisture can be further quantified with the help of imaging techniques.

The heat of reaction, as obtained from *in-situ* DSC

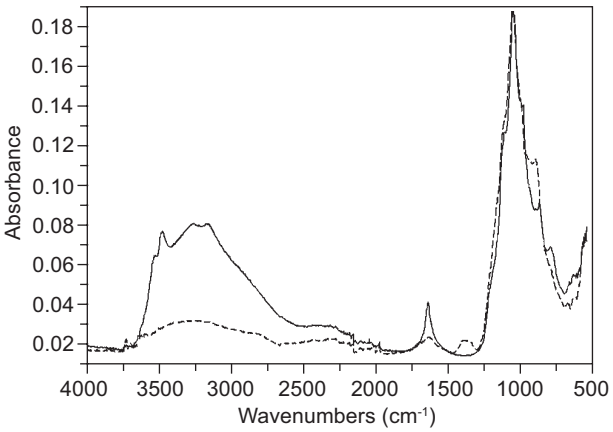

Figure 2. IR spectra of IPC sample cured at 40°C for 24 h showing brushite to monetite transformation (solid line: before TMA experiment, dashed line: after TMA experiment).

Table 1. Effect of curing temperature and curing time on CTE values.

Curing Conditions	CTE values ($\times 10^{-6}$) (K^{-1})
24 hr 40°C	7.78
48 hr 40°C	7.95
72 hr 40°C	8.10
24 hr 60°C	8.43
48 hr 60°C	8.62
72 hr 60°C	9.05
24 hr 80°C	8.88
48 hr 80°C	12.05
72 hr 80°C	9.77

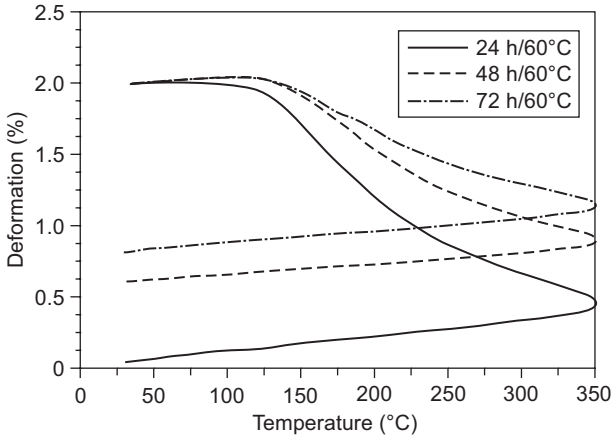

Figure 3a. TMA results of IPC samples with variation in curing time, for a given curing temperature of 60°C.

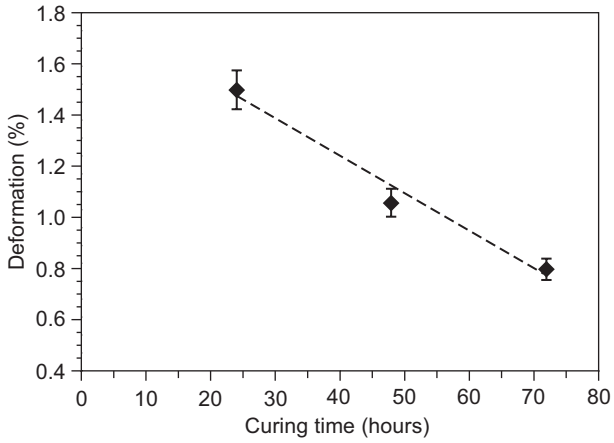

Figure 3b. Deformation values (%) as obtained from the first heating cycle of TMA experiments plotted against various curing times (hours) showing linear trend, for a given curing temperature of 60°C.

measurements (Figure 4), were also correlated with the curing conditions. For four different isothermal curing temperatures, Table 2 enlists the amount of heat released (the area under the DSC curve) during cement hydration and the time up to which this exothermic process was extended. The DSC results show that all specimens undergo an exothermic setting process, but with different enthalpies of reactions and there are no remaining endo- or exo-thermic reactions after the setting of the cement.

The heat of hydration for IPC formation was found to be in the range of 24.71 − 87.61 J g^{-1} or W·s·g^{-1} (Table 2), which is much less than that of the Ordinary Portland cement (OPC), usually 500 J·g or W·s·g^{-1}. IPC has a much shorter setting time than OPC (1 - 6 hours vs. 28 days), which can be attributed to higher porosity and hence higher water permeability in OPC. Furthermore, IPCs do not require aggregates, which is important for applications where light weight is required.

Wollastonite is not used as a reinforcing filler here, rather it is involved in the chemical reaction. When the phosphoric acid formulation and the Wollastonite powder mixture are stirred, the sparsely alkaline oxides dissolve and an acid-base reaction is initiated. The result is a slurry that hardens into a ceramic product. The setting is the result of gelation by salt formation and the Ca^{2+} cations are extracted from the calcium silicate. These cations react with the phosphate anions within the solvent and form a precipitate of salt molecules. Under proper conditions mainly controlled by the pH, these molecules form an ordered structure that grows into crystals that confirm IPC formation [23].

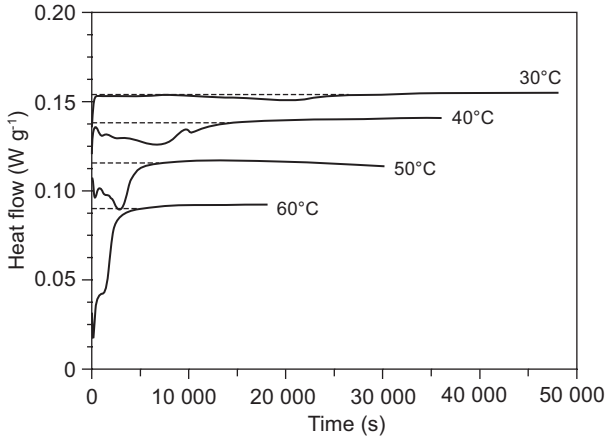

Figure 4. DSC results showing variation in heat of cement hydration and time for completion as a function of curing temperature (30, 40, 50 and 60°C), curves are stacked over one another for clarity.

Table 2. Heat released and time taken for cement hydration as a function of curing temperature.

Cure temperature (°C)	Heat released (W·s·g^{-1} or J·g^{-1})	Time taken for the exothermic process (sec)
30	24.71	19944.00
40	74.66	6834.50
50	77.22	6533.15
60	87.61	4299.94

From the shape of the DSC curves, it is apparent that the cement hydration included five periods [27]: starting period (A), induction period (B), accelerating period (C), decelerating period (D), and terminating period (E). In the starting period, water was absorbed and then imbibed the surface of the grains upon mixing calcium silicate powder with water present in the aqueous phosphoric acid solution. This is a physical exothermic process. In the induction period, the particle dissolution contributed to a rise in concentration of the Ca ions in the solution. The accelerating period is a fast reaction rate controlling region, which is subsequently used for activation energy calculation. In this step, the phosphate anions react with the newly released Ca cations and form a coordinated network. In the decelerating period, hydration reaction decreased and the reaction process converted from the surface controlled to diffusion controlled process after the hydrate product grew around the particle surface of the raw materials. The hydrate product layer was finally destroyed by crystallization interior stress.

Figure 4 shows that with decrease in curing temperature, the hydration rate (heat flux) decreased and the reaction time was increased, causing the reaction peak to shift forward. In other words, the increase in curing temperature not only makes the reaction advance but also enlarges it. The second period (induction period) was shortened as the curing temperature rose.

Particle size of the raw material, ratio of calcium to phosphate [27] and presence of retardant [28-30] are known to affect the hydration process. These parameters were kept constant in this study, so that the effect of curing condition on cement hydration can be studied in isolation.

Model-free Friedman analysis, based on Equation 2, was used to see how the reaction extent varied with curing condition and the activation energy was quantified to a fairly good approximation. The linear slope in accelerating period of the DSC curve (Figure 4) represented the reaction rate, α in Figure 5. Q_i and Q_f of equation (3) was determined from the start and end point of the rate-determining accelerating period (C), therefore ignoring early build up of hydrates that may take place during the starting period (A) of the hydration. Using equation (3), degree of hydration (α) was calculated at various times in the accelerating region. A specimen curve of α versus time in accelerating period, for a cure temperature of 50°C, is shown in Figure 5. The slope of this curve is essentially ($d\alpha/dt$). Substituting the values of ($d\alpha/dt$) and T in Equation 2, the activation energy can be obtained from the slope of the plot of $-ln(d\alpha/dt)$ vs. $1/RT$ (Figure 6). The hydration activation energy was found to be 57.8 kJ mol^{-1}.

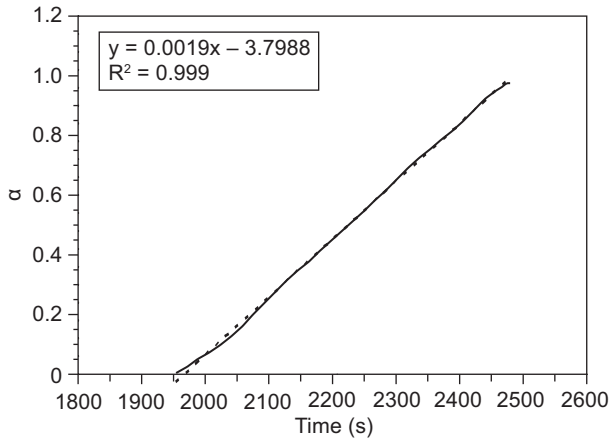

Figure 5. Rate of hydration (α) vs. time (sec) valid for the accelerating period of cement hydration at a given cure temperature of 50°C (solid line: experimental data and dotted line: linear fit).

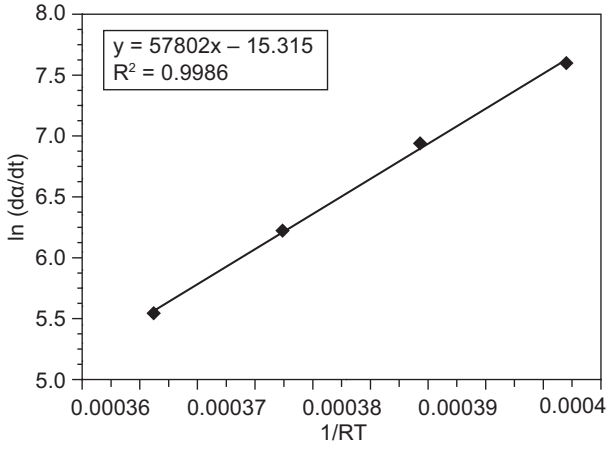

Figure 6. Activation energy of cement hydration from the plot of -ln(*dα*/*dt*) vs. 1/*RT*.

CONCLUSIONS

The knowledge of thermal properties is critical in evaluating the performance of a concrete material. This study shows that curing condition can play a vital role in optimizing the thermal properties of IPC materials. The effect of cure temperature and cure time on thermal properties of a wollastonite-based calcium phosphate cement was studied. A mass loss of 11.7 % at 105 – 220°C and 1.8 % at 380 − 500°C was attributed to brushite to monetite and monetite to calcium pyrophosphate transformation, respectively; which was further confirmed by FTIR. TGA results also indicated that the mass loss can be minimized by increasing curing time and decreasing curing temperature. Deformation values recorded from the first heating cycle of TMA results revealed a linearly decreasing trend with increase in curing time and was somewhat reduced with increase in cure temperature. CTE values, as obtained from the second heating cycle of TMA results remained more-or-less constant with variation in curing time and slightly increased with increase in cure temperature, possibly due to change in moisture content. From the (exothermic) DSC curves it was apparent that a decrease in curing temperature, caused a decrease in heat of reaction and an increase in reaction time. Rate of hydration for different cure temperatures were evaluated from the linear slope in the accelerating period of cement hydration and the data was matched with a model-free Freidman analysis. The activation energy was found to be 57.8 kJ·mol^{-1}. This type of calcium phosphate cement with lower heat of hydration and lower setting time seems to be a sustainable alternative to conventional cement materials.

Acknowledgment

The author would like to thank Johan Blom, in the Department of Mechanics of Materials and Construction, for preparing the moulds.

REFERENCES

1. Davidovits J.: *Geopolymer Chemistry and Applications*, Geopolymer Institute, Saint Quentin 2008.
2. Tchakoute Kouamo H., Mbey J.A., Elimbi A., Kenne Diffo B.B., Njopwouo D.: Ceramics International *39*, 1613 (2013).
3. Olivia M., Nikraz H.: Materials & Design *36*, 191 (2012).
4. Alshaaer M., Cuypers H., Mosselmans G., Rahier H., Wastiels J.: Cement and Concrete Research *41*, 38 (2011).
5. Alshaaer M., Cuypers H., Rahier H., Wastiels J.: Cement and Concrete Research *41*, 30 (2011).
6. Tofighi A., Schaffer K., Palazzolo R.: Key Engineering Materials *361-363*, 303 (2008).
7. Brown W.E., Chow L.C.: *62*, 672 (1983).
8. Flautre B., Descamps M., Delecourt C., Blary M.C., Hardouin P.: Journal of Materials Science: Materials in Medicine *12*, 679 (2001).
9. Komath M., Varma H.K.: Indian J. Dent. Res. *15*, 89 (2004).
10. Ambard A.J., Mueninghoff L.: J. Prosthodont. *15*, 321 (2006).
11. Guo H., Wei J., Yuan Y., Liu C.: Biomed. Mater. *2*, S153 (2007).
12. Horstmann W.G., Verheyen C.C., Leemans R.: Injury *34*, 141 (2003).
13. Hofmann M.P., Gbureck U., Duncan C.O., Dover M.S., Barralet J.E.: J. Biomed. Mater. Res. B Appl. Biomater. *83*, 1 (2007).
14. Liverneaux P.: Rev. Chir. Orthop. Reparatrice Appar. Mot. *89*, 532 (2003).
15. Link D.P., van den Dolder J., Jurgens W.J.F.M., Wolke J.G.C., Jansen J.A.: Biomaterials *27*, 4941 (2006).
16. Li M., Liu X., Liu X., Ge B.: Clin. Orthop. Relat. Res. *468*, 1978 (2010).
17. Chew K-K., Low K-L., Zein S.H.S. et al.: Journal of the Me-

chanical Behavior of Biomedical Materials *4*, 331 (2011).
18. Krüger R., Groll J.: Biomaterials *33*, 5887 (2012).
19. dos Santos L.A., de Oliveira L.C., da Silva Rigo E.C. et al.: Artif. Organs *24*, 212 (2000).
20. Xu H.H., Quinn J.B.: Biomaterials *23*, 193 (2002).
21. Pan Z., Jiang P., Fan Q., Ma B., Cai H.: J. Biomed. Mater. Res. B Appl. Biomater. *82B*, 246 (2007).
22. Matsuzaki A., Nagoshi M., Noro H., Yamashita M., Hara N.: Materials Transactions *52*, 1244 (2011).
23. Wagh A.S.: *Chemically bonded phosphate ceramics*, Elsevier Science, New York 2004.
24. Adolfsson D.: *Cementitious properties of steelmaking slags*, Doctoral thesis, Luleå University of Technology, Sweden 2011.
25. Brown P.W., Pommersheim J.M., Frohnsdorff G. In: *Cements Research Progress*, p. 245-260, Ed. J. F. Young, The American Ceramic Society, Columbus 1983.
26. Aligizaki K.K.: *Pore structure of cement-based materials: testing, interpretation and requirements*, CRC Press, Boca Raton 2005.
27. Liu C., Gai W., Pan S., Liu Z.: Biomaterials *24*, 2995 (2003).
28. Yang J., Qian C.: Journal of Wuhan University of Technology-Mater. Sci. Ed. *25*, 613 (2010).
29. Yang Q., Wu X.: Cem. Concr. Res. *29*, 389 (1999).
30. Sarkar A.K.: Ceram. Bull. *69*, 234 (1990).